Electronic Supplementary Material (ESI) for Soft Matter.

Supplementary Information

Precise Morphology Control and Fast Merging of Complex Multi-Emulsion System: the Effects of AC Electric Fields

Yi Huang [a] ¶, Shuai Yin [a] ¶, Wen Han Chong, Teck Neng Wong [a]**, Kim Tiow Ooi

¶ These two authors contribute equally.

[a]*School of Mechanical and Aerospace Engineering, Nanyang Technological University. 50 Nanyang, Avenue, Singapore 639798*

General setup of the experimental system

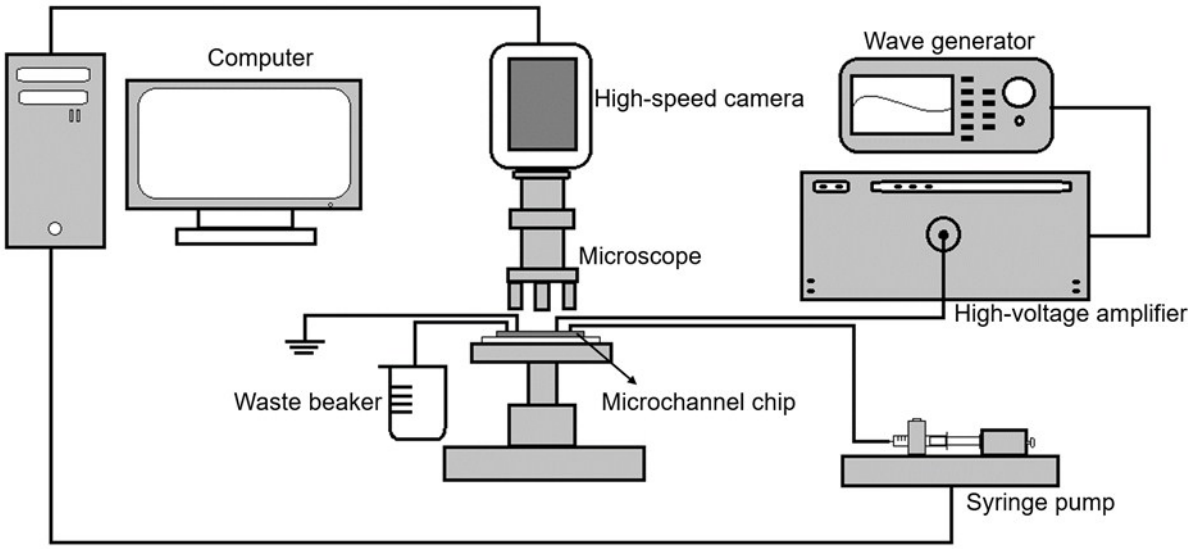

Fig. S 1 General setup for the experiments.

The experimental setup is shown in Fig. S 1. The microchannel chip is placed on the microscope platform, where the result is observed under an inverted microscope (Leica DM ILM) and recorded by a high-speed camera (Phantom V611, 6200 FPS at the full resolution of 1280×800). The record data can be replayed and stored by the computer. The high-precision syringe pump system (Centoni neMESYS) is connected to the chip to control the flow rate of each fluidic sample, which can be controlled by the computer. The waste fluid comes from the microchannel is collected by a waste beaker.

The high voltage supply system consists of a waveform generator (Agilent 33500 B) and a high voltage amplifier (Treck 5/80). The waveform generator is able to generate the on-demand Sine electric signal with specific voltage amplitude and frequency, which is then amplified by the amplifier (Treck 5/80) to reach required field strength. The obtained electric field will be delivered to the electrodes connected. Thus, this external electric field setup enables us to apply AC electric field around the second junction of the microchannel.

Microchannel geometries and configurations

O/W/O double emulsions

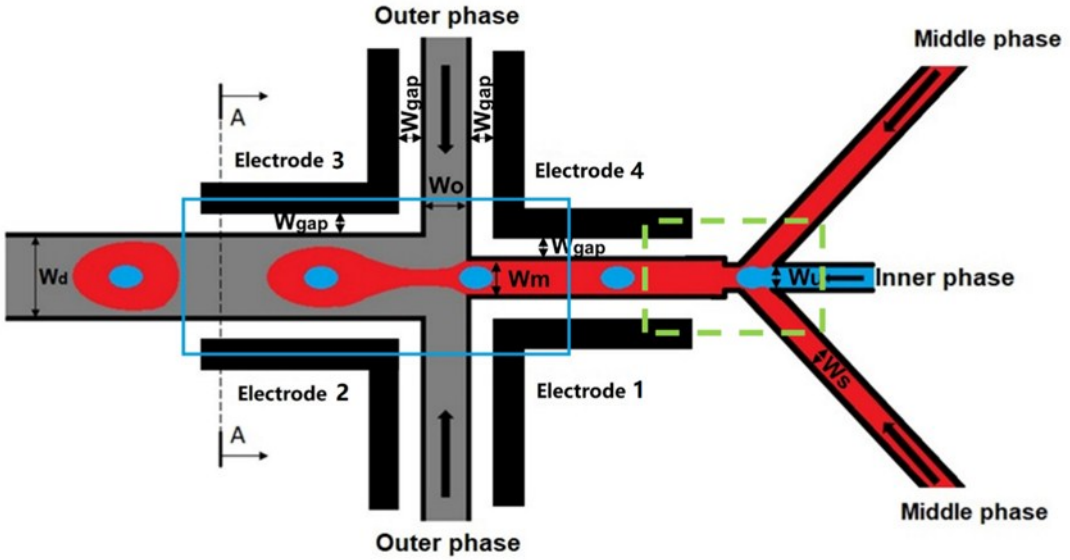

Fig. S 2 Top diagram of the microchannel. (The part in dash box is the first junction area, the part in the solid box is the second junction area)

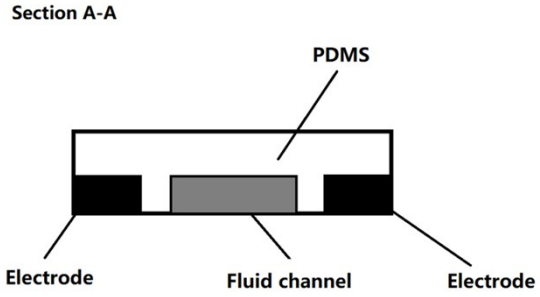

Fig. S 3 The A-A section view of the microchannel.

The channel structure in the red dashed box is shown in Fig. S 2. The microchannel is an axial symmetry geometry. Fig. S 3 is the section view of the channel and the electrodes. All channels have the height of 55 μm. The double emulsion is formed through hierarchical flow-focusing microchannel. Before the first junction, the inner phase flows in the center channel while the middle phase flows in the first two side channels. At the first junction (the dashed box in Fig. S 2), the single emulsion droplet is formed. The outer phase is pumped into the chip and go through the second two side channels to reach the second junction (the full line box in Fig. S 3). The middle phase pinch-off and thus the double emulsion is formed.

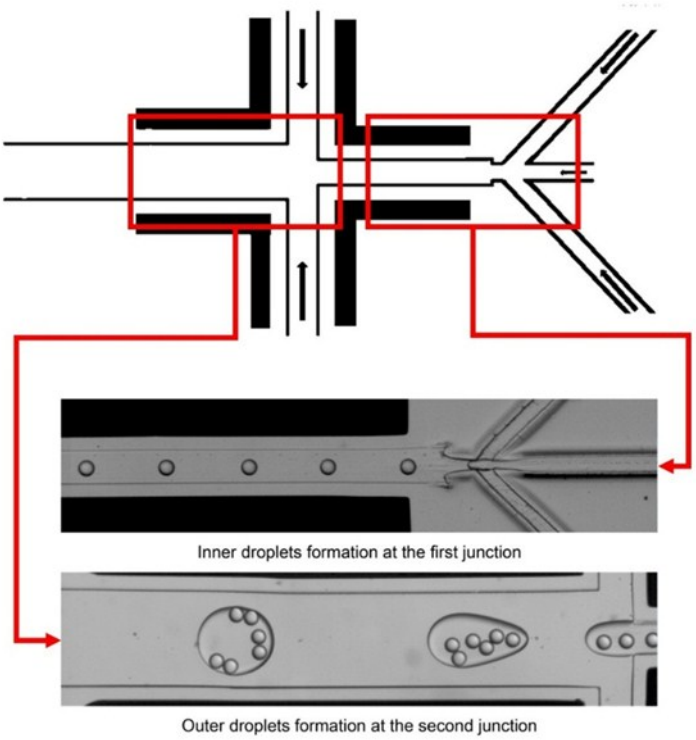

Fig. S 4 The inner droplet and the outer droplet formations in the microchannel.

When the flow rate conditions of the three fluids are fit with each other, the stable formation of O/W/O double emulsion could be reached. The oil in water droplets formed at the first junction with a stable generation rate. The middle phase broke up at the second junction and capsulated inner drops (cores) inside, thus the O/W/O double emulsion formed. Figure 3.6 shows the formation process of the inner drops and the double emulsions at the first junction area and the second junction area respectively. At the first junction, the inner phase breaks up and become the inner droplets in middle phase. At the second junction, the middle phase containing inner droplets breaks up and turns to the outer droplets, and the outer phase is the continuous phase.

By adjusting the flow rates of the three fluids, the sizes of inner drops and the outer drops can be controlled. Besides, the number of inner drops inside the outer drops can also be changed by the same way. The black areas in the Figure 3.6 are the electrodes.

O/W/O double emulsion formation under tangential configuration---other results

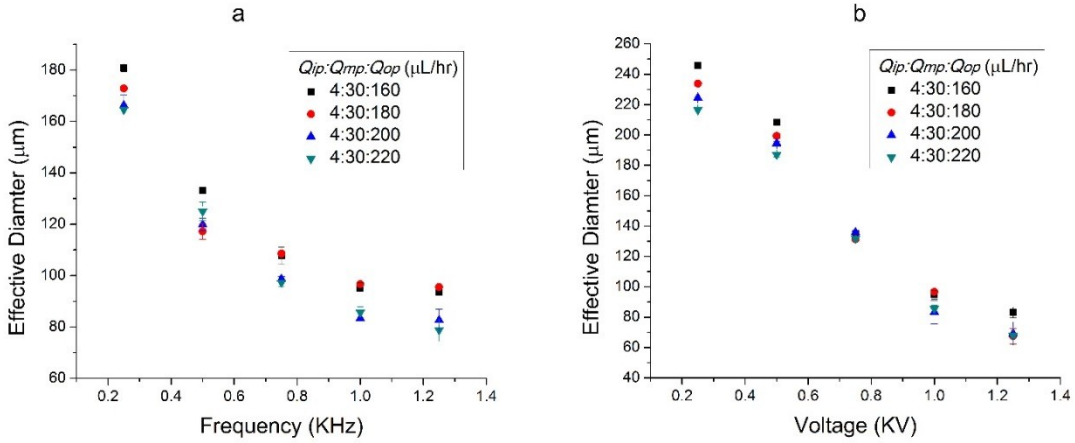

Fig. S 5 The change of the effective diameter of outer droplets with different outer phase's flow rates over the different (a) frequencies (*V*=1 KV) and (b) voltages (*f*=1 KHz)

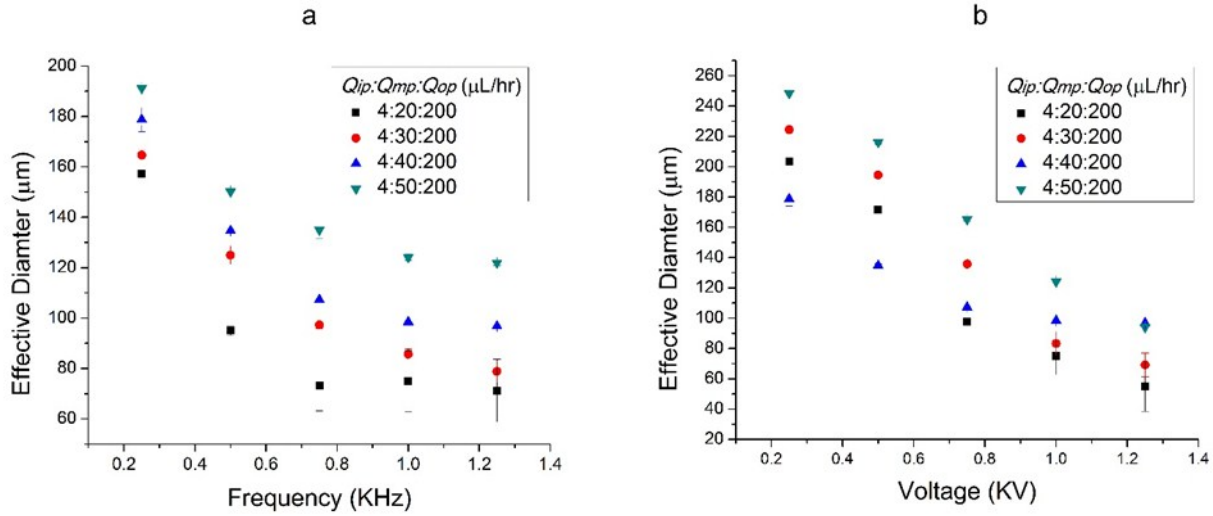

Fig. S 6 The change of the effective diameter of outer droplets with different middle phase's flow rates over the different (a) frequencies (*V*=1 KV) and (b) voltages (*f*=1 KHz).

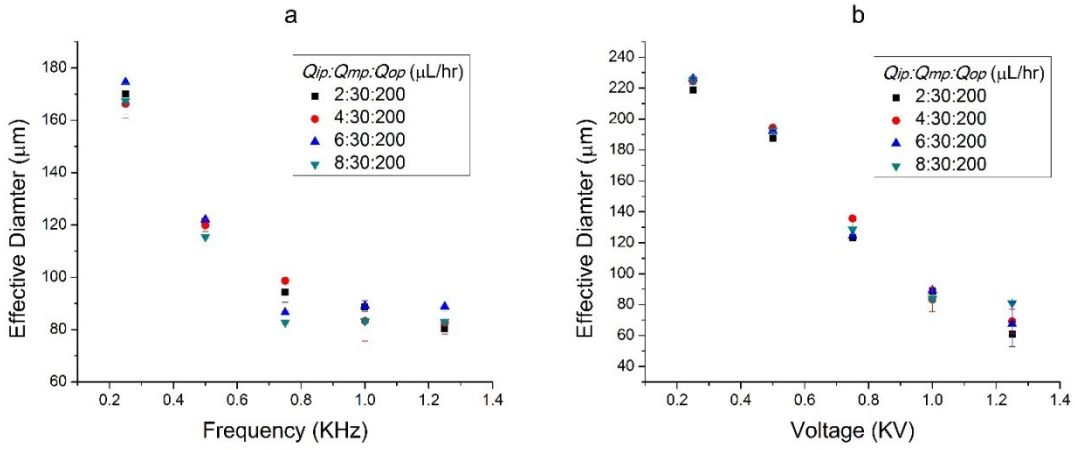

Fig. S 7 The change of the effective diameter of outer droplets with different inner phase's flow rates over the different (a) frequencies (*V*=1 KV) and (b) voltages (*f*=1 KHz).

W/O/W double emulsions configurations

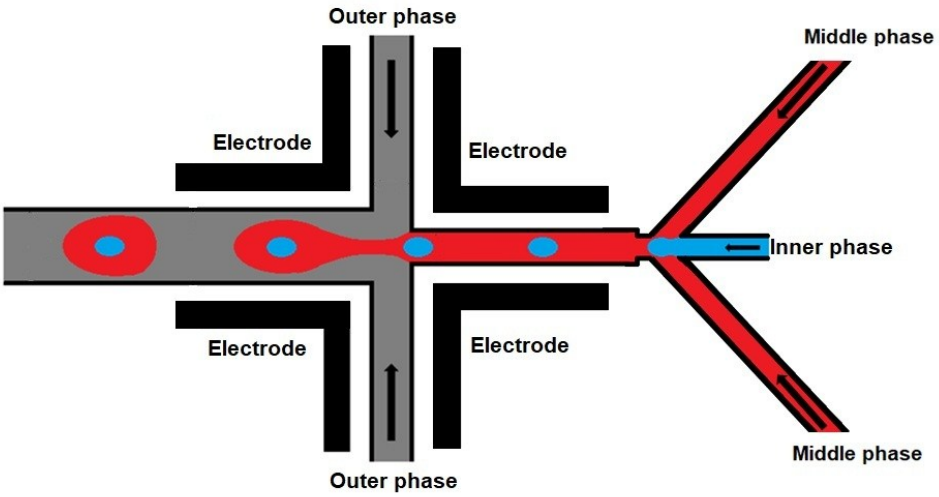

Fig. S 8 Schematic diagram of the microchannel of Structure 1 for formation of W/O/W double emulsion with single-type cores.

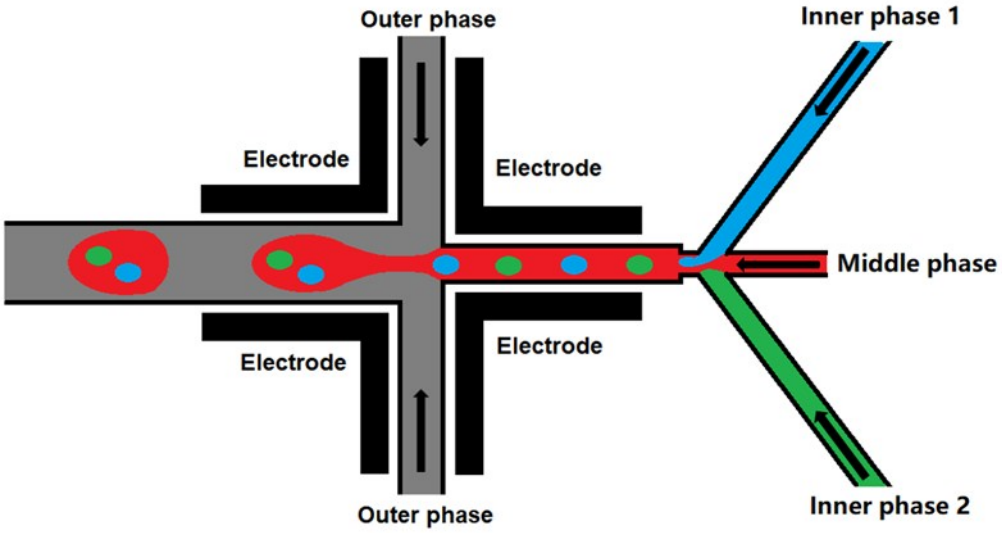

Fig. S 9 Schematic diagram of the microchannel of Structure 2 for formation of W/O/W double emulsion with double-type cores.

Two-step merging---other conditions

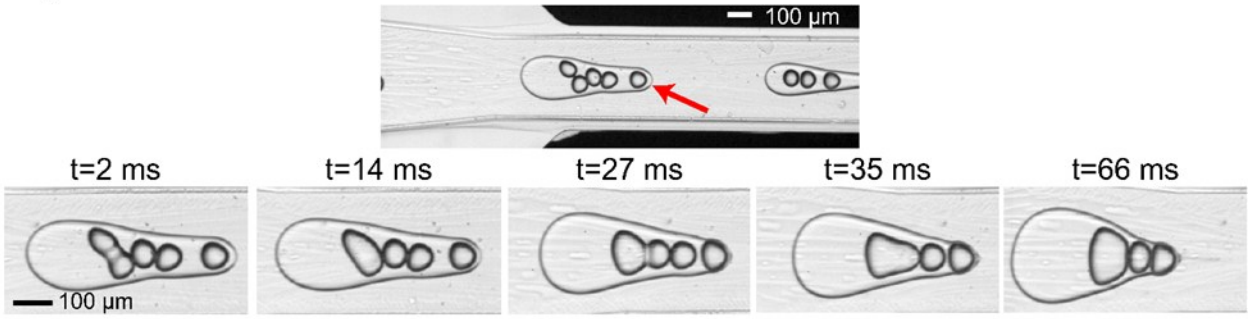

Fig. S 10 The coalescence between inner droplets in double emulsions. The conditions for each cases Q_{ip}:Q_{mp}:Q_{op}=15:50:400 μL/hr, *V*=1.2 KV, *f*=1 KHz.

In addition with the situation presented in the main article, Figure 4 (b), we have also achieved the two-step merging with multi cores inside the W/O/W double emulsions. As shown in Fig. S 10, 3 of the initial 5 core becomes one core through the two-step merging leaving the other two cores untouched.

Merging dynamics of the core and mixing characteristics under the AC field

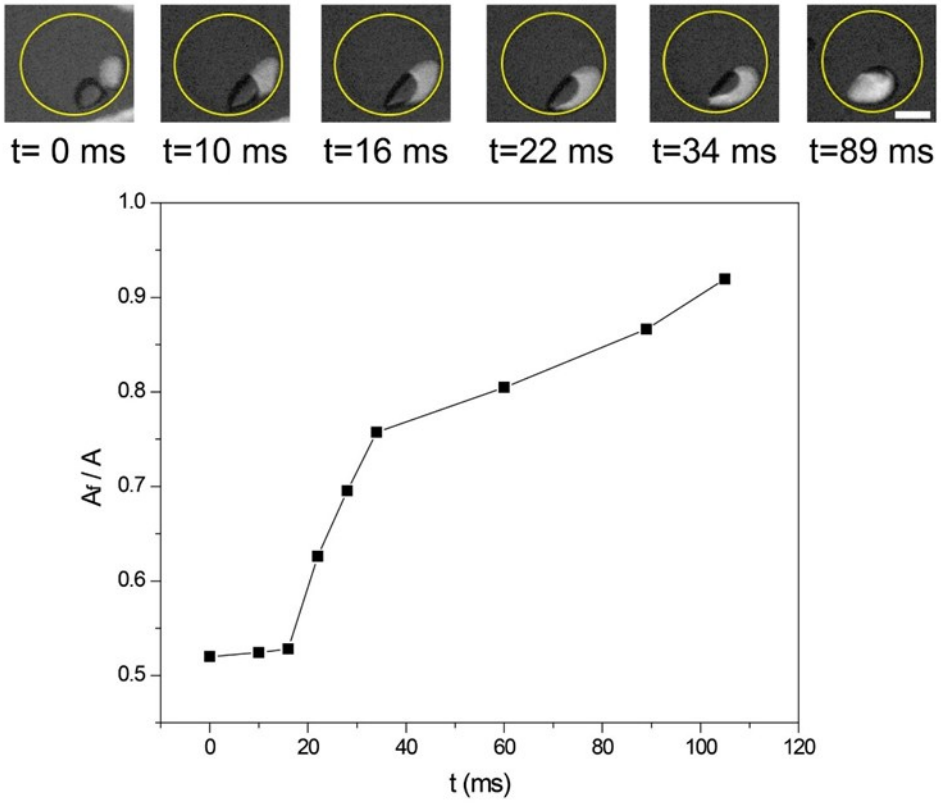

Fig. S 11 The coalescence process of two inner droplets and the change of the ratio of the dye area (A_f) and the coalescence droplets area (A) over the time; Q_{ip1}:Q_{ip2}:Q_{mp}:Q_{op}=5:2:25:270 μL/hr; V_0=1.3 KV, fe=1 KHz; (scale bar: 50 μm).

The images in Fig. S 11 show the coalescence process of the inner droplets within an outer droplet after the second junction. The interface between the middle phase and the outer phase is represented by the yellow circle lines in the images. The dye mixing efficiency during the coalescence is characterized by the change of the ratio of the dye area (A_f) and the coalescence droplets area (A) over time. At t=10 ms, the coalescence starts, a part of interfaces of the two inner droplets merge together, and at t=105 ms, A_f/A reaches 92%. The time needed for the coalescence is about 100ms. The flow rate condition is: Q_{ip1}/ Q_{ip2}/Q_{mp}/Q_{op} = 5/2/25/270 μL/hr. The conditions for the electric field are: *V*=1.3 KV, *f*=1 KHz.

Microchip Fabrications

Lithographic method

We employ the lithographic method for engraving the design on to the silicon wafer, where we adopt a negative photoresist Su8 from Microchem. Followed by the polydimethylsiloxiane (PDMS, Dow Corning Sylgard 184) filling and curing process, the design of the structures are successfully imprinted into the PDMS layer. Next, we demold the PDMS layer from the silicon wafer and conduct the oxygen plasma bonding with one slice of microscopy glass substrate spin coated with one thin layer of PDMS to ensure uniform surface properties. The microchip is finalized by placing into an oven for 2 hours heating at temperature of 120 ˚C to stabilize the surface property.

Controlled surface modification

Thus, a surface treatment process at specific position of microchannel is necessary for producing the double emulsion. In the process of surface treatment, a uniform grafted surface is necessary for stable formation of drops. In our experiments, the benzophenone acted as a photo-initiator and was diluted in acetone. This solution was firstly injected into the microchannel. Next step was loading the acrylic acid in water solution into the channel, and treated it with UV light for 2-3 minutes. This method is efficient and able to bring a durable surface hydrophilic transition to the PDMS channel.

For the O/W/O double emulsion formation, the surface treatment was conducted at the first junction to cover the O/W droplet formation area, while for the W/O/W double emulsion formation, the second flow focusing junction is modified.

Materials and properties

Materials

O/W/O double emulsion

For O/W/O double emulsion formation, the mineral oil with 0.3 wt% of non-ionic surfactant (Span 80, Sigma Aldrich) is used as the inner phase. The DI water with 65 wt% of Glycerol is used as the middle phase and the Mineral Oil with 5 wt% of Span 80 is the outer phase. The Span 80 is used for assistant droplet formation and avoiding the droplet coalescence. The Glycerol in DI water is meant for facilitating droplet formation. The details are listed in Table S

Table S 1 O/W/O double emulsion fluids

Phase	Fluid
Inner phase	Mineral oil with 0.3 wt% Span 80
Middle phase	DI water with 65wt% Glycerol
Outer phase	Mineral oil with 5 wt% Span 80

W/O/W double emulsion

Table S 2 Materials for generation of W/O/W double emulsion in Structure 1 (Fig. S 8).

Phase	Fluid
Inner phase 1	DI water with 2 wt% Tween 20
Middle phase	Mineral oil with 0.3 wt% Span 80
Outer phase	DI water with 70 wt% Glycerol, 0.3 wt% SDS

Table S 3 Materials for two-type cored W/O/W double emulsion in Structure 2 (Fig. S 9).

Phase	Fluid
Inner phase 1	DI water with 2 wt% Tween 20
Inner phase 2	DI water with 2 wt% Tween 20 and 4mmol/L Rhodamine 6G
Middle phase	Mineral oil with 0.3 wt% Span 80
Outer phase	DI water with 70 wt% Glycerol, 0.3 wt% SDS

For W/O/W double emulsion formation in Structure 1, the DI water with 2 wt% surfactant (Tween 20, Sigma Aldrich) was used as the inner phase, the Mineral Oil with 0.3 wt% Span 80 was used as the middle phase, the DI water with 70wt% Glycerol and 0.3 wt% surfactant (Sodium dodecyl sulfate, Sigma Aldrich) was the outer phase. Structure 2 allows two different types of inner phases to form the droplets at the first junction. Fluorescence dye was used to distinguish the two inner phases, Rhodamine 6G was added to one inner phase of DI water with Tween 20. Table S 2 and 3 show the fluids adopted.

Interfacial intension measurement

Table S 4 Interfacial tension characterizations for the O/W/O systems adopted in the experiments

No.	Two fluidic samples that form the interface	Interfacial tension (mN/m)
1	DI water with 65wt% Glycerol	5.300±0.072
	Mineral oil with 5 wt% Span 80	

The interfacial tension are measured by the tensiometer, model: FTA 200, using pendent droplet method. We measured the interfacial tension for at least three times to ensure the repeatability.

Dielectric constant of the fluids (relative electric permittivity)

Table S 5 dielectric constant of the fluids

Fluids	Relative permittivity ε_r
Mineral oil with 5% span 80	2.8

The dielectric constants of the fluids are measured by filling the fluids into a self-fabricated capacitor of cylindrical shape. The capacitances with and without the fluids are measured by a precision LCR meter (Keysight E4980AL). The relative permittivity can then be calculated by the formula of $C = \varepsilon_0 \varepsilon_r A / d$.

Calculation of the electric capillary number

The electric capillary number is defined as $Ca_E = \varepsilon_{OP} E^2 a / \sigma$, where $\varepsilon_{OP} = 2.8 \times 8.85 \times 10^{-12}$ F/m (Table S 5) stands for the electric permittivity of the outer phase, the interfacial tension $\sigma = 5.3$ mN/m (Table S 4), a represents the characteristic length and the electric strength E can be calculated as $E = (V / 2\sqrt{2}) / (2W_{ga} + W_{ch})$, for tangential electric configuration $W_{ch} = 100$ μm while for the normal configuration $W_{ch} = 300$ μm.

The detailed parameters are listed in Table S 6 and Table S 7.

Table S 6 Parameters for calculation of electric capillary number under tangential configuration

Voltage (P-P)/ V	$2W_{ga} + W_{ch}$ / μm	a (Char. Len.) / μm	σ Interfacial tension/ mN·m^{-1}	The electric capillary number Ca_E
0	200	100	5.30	0.00E+00
500	200	100	5.30	3.65E-01
750	200	100	5.30	8.22E-01
1000	200	100	5.30	1.46E+00
1250	200	100	5.30	2.28E+00

Table S 7 Parameters for calculation of electric capillary number under normal configuration

Voltage (P-P)/ V	$2W_{ga} + W_{ch}$ / μm	a (Char. Len.) / μm	σ Interfacial tension/ mN·m^{-1}	The electric capillary number Ca_E
500	400	300	5.30	2.74E-01
750	400	300	5.30	6.16E-01
1000	400	300	5.30	1.10E+00
1250	400	300	5.30	1.71E+00

Verification of the analysis approach---the effective diameter

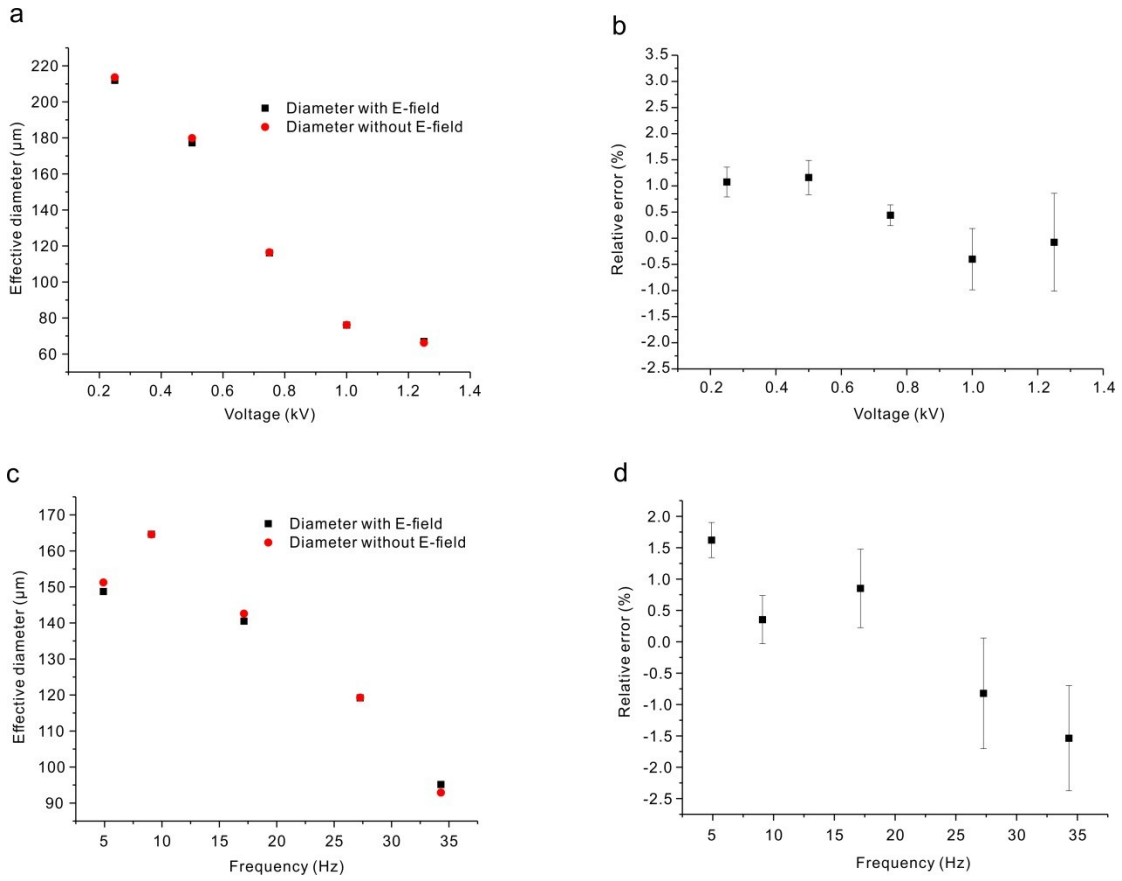

Fig. S 12 Verification of the effective diameter for the electric fields in the tangential direction. (a), (c) Effective diameters with and without electric fields (after it is stabilized) considering various voltages and frequencies respectively, (b), (d) are the corresponding relative errors occurred by adopting the effective diameter for different voltages and frequencies, respectively.

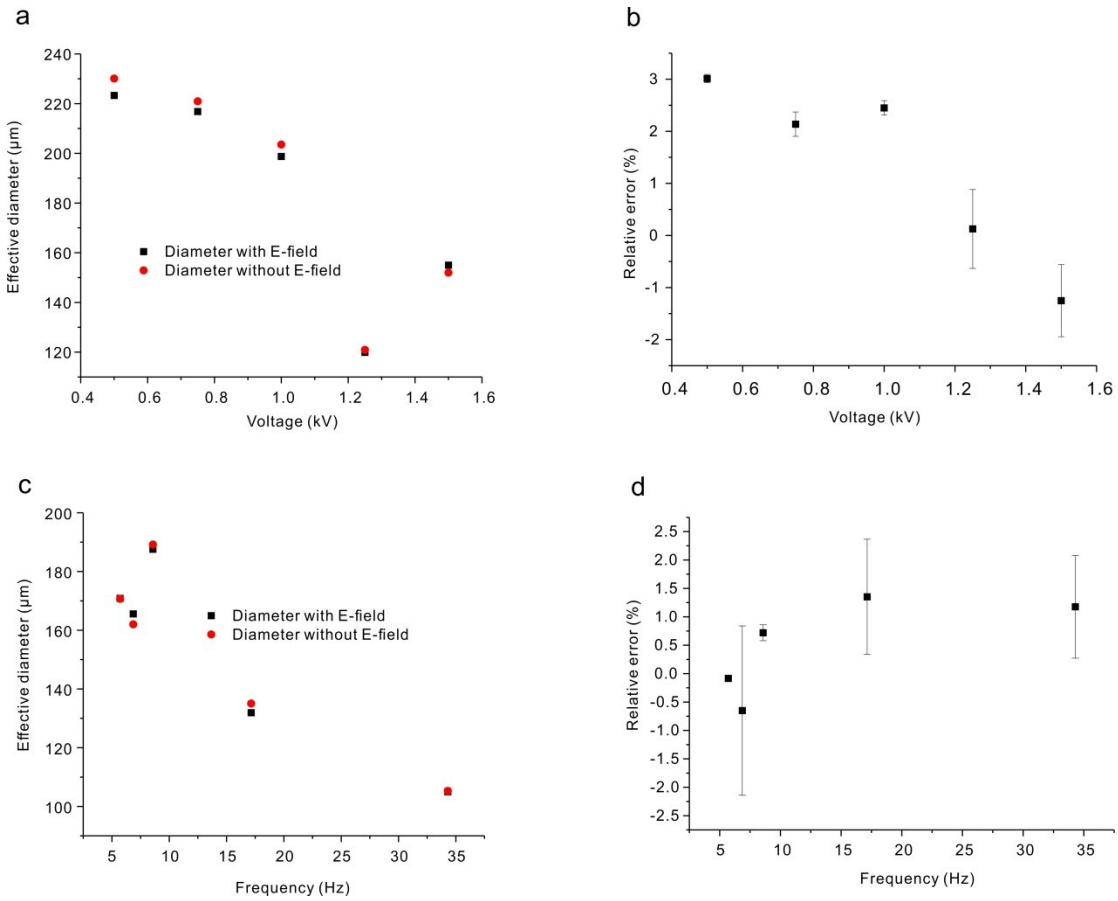

Fig. S 13 Verification of the effective diameter for the electric fields in the normal direction. (a), (c) are the measured effective diameter with and without electric field (after it is stabilized) of various voltages and frequencies respectively, (b), (d) are the corresponding relative errors induced by adopting the effective diameter respectively.

It is seen from the results in both the Fig. S 12 and Fig. S 13, the relative error occurred are limited, less than 2%, considering various conditions, including the direction (tangential and normal), the voltage and the frequency of the electric field. The result shown verifies our analysis approach.

List of videos

No.	File name	Remarks
1	S 1. Tang. Field OWO	Effects of the of **tangentially** applied AC fields on O/W/O double emulsions
2	S 2. Normal. Field OWO	Effects of the of **normally** applied AC fields on O/W/O double emulsions
3	S 3. 1 KV 1 KHz two core merging OWO	Two-core merging
4	S 4. 1250 V 1 KHz three core merging OWO	Three-core merging
5	S 5. 1.3kv 1khz two core merging fluorescence OWO	Merging of two different cores under fluorescent microscopy configurations
6	S 6. 1.25 KV 1 KHz droplet-double emulsion merging OWO	Merging of a single droplet with a double emulsion
7	S 7. 1 KV 0.75 KHz two double emulsion merging OWO	Merging of two double emulsions
8	S 8. 600V 1Khz core extraction WOW	**Extraction** of the cores achieved by the AC field in W/O/W double emulsions.